ACADEMIA ROMÂNĂ
Revue Roumaine de Chimie
http://web.icf.ro/rrch/

Rev. Roum. Chim.,
2020, *65*(3), 255-268
DOI: 10.33224/rrch.2020.65.3.05

SPECTRO-ANALYTICAL, ANTIMICROBIAL AND ANTITUMOR STUDIES OF THE FIRST AND SECOND GENERATION OF CEPHALOSPORIN COMBINED WITH RUTHENIUM(III) ION AS A DRUG MODEL

Lamia A. ALBEDAIR,[a,*] Samar O. ALJAZZAR,[a] Amani S. ALTURIQI,[a]
Mohamed I. KOBEASY[b,c] and Moamen S. REFAT[c,d,*]

[a] Department of Chemistry, College of Science, Princess Nourah bint Abdulrahman University, Riyadh 11671, KSA
[b] Department of Biochemistry, Faculty of Agriculture, Cairo University, Giza, Egypt
[c] Department of Chemistry, Faculty of Science, Taif University, Al-Hawiah, Taif, P.O. Box 888 Zip Code 21974, Saudi Arabia
[d] Department of Chemistry, Faculty of Science, Port Said University, Port Said, Egypt

Received December 2, 2019

Two new ruthenium(III) complexes of 1st (cefradine) and 2nd (cefoxitin) generation of cephalosprin drugs have been synthesized and well characterized based on physical (molar conductance), spectral (FTIR & UV-Vis), thermal analysis (TGA & DTA) and analytical data. Both cefradine (ceph-1) and cefoxitin (ceph-2) act as a bidentate ligand and the synthesized complexes $[Ru(L)(Cl)_2(H_2O)_2]$ where [L=cefradine and cefoxitin] are showing octahedral geometry. The analytical data refer to 1:1 (Ru^{3+}/ceph) stoichiometry. FTIR analysis confirmed the coordination through the two oxygen atoms of β-lactam and carboxylate groups. The surface morphology and particle size investigations were evaluated using XRD, SEM and TEM analyses. The antimicrobial effect of ruthenium(III) ion upon complexity with ceph-1 and ceph-2 were assessed against Gram positive (*Staphylococcus epidermidis* & *Staphylococcus aureus*) and Gram negative (*Klebsiella* spp., *Escherichia coli*) bacterial strains. The potential anticancer properties of Ru^{3+} cephalosprin complexes were evaluated in *vitro* on colorectal adenocarcinoma (Caco-2) and breast cancer (MCF-7) cell lines, indicating that the synthesized Ru(III) complexes are relatively better cytotoxic agents in comparison with cisplatin standard drug.

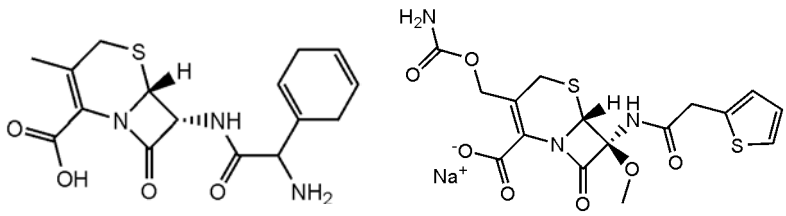

INTRODUCTION

Antibiotics of cephalosporins (cephs) have become a major part of prescription antibiotics for hospitals in rich countries. Cephalosporins are classified by generation. They are prescribed for a wide range of infections every day. There is no doubt that popularity depends on less sensitivity and toxicity risks as well as a wide range of activity.[1] Cephalosporins are the most common category from antibiotics they are structurally and pharmacologically linked Penicillin. Like cephs penicillin have a beta-lactam ring structure that interferes with the synthesis of the bacterial cell wall and this is called a bactericide. In general, low-generation cephs are more G+ activity and higher-generation cephs more G– activity. The 4th generation drug cepepime is an exception, with G+ activity equivalent to the 1st generation and G– activity equivalent to the 3rd generation cephs.[2] The 3rd generation cephs are less active against G+ cocci. Extensive ceph class restriction significantly reduced nosocomial, plasmid-mediated, ceph-resistant Klebsiella infection and colonization.[3]

* Corresponding author: msrefat@yahoo.com

The 1st generation cephs have a bacterial efficient against G+ cocci and less active against G– bacteria.[4] Regarding 2nd generation cephs, there have a higher efficiency against G– bacteria but are lesser active than 3rd and 4th generations.[5,6] In literature survey, the ceph-metal chelations were isolated in solid form with 1:1[7] or 2:1 molar ratio[8,9] in *situ* CH_3OH[5,6] or in dist. H_2O.[10] There are several cephs drugs acts as a good chelating agent towards different metal ions like cefoxitine,[6] ceftriaxone,[5] cefradine,[10] cefixime,[11] cephalothine,[12] cefotaxime, cefalaxin, cephamandole, ceftazidime, cephapirin,[13] ceforuxime,[14] cefadroxil, cefoperazone,[15] cefaloridine,[13] cefdinir,[16] cefazolin[16,17] and cefaclor.[18]

According to the vital efficiency of ruthenium compounds against microbial organism and cancer cells,[19–21] therefore herein in this article, a chemical structures and biological evaluations of the Ru(III) complexes of cefradine (Fig. 1_a) and cefoxitin sodium (Fig. 1_b) have been reported.

EXPERIMENTAL

1. Chemical

The chemicals $RuCl_3.xH_2O$, cefradine and cefoxitin sodium were received from Aldrich chemical company (United States) and used without further purification. The solvents were used have an analytical grade.

2. Synthesis of Ru(III) cephs complexes

A 50 mL methanolic solutions of cefradine and cefoxitin sodium (1 mmol) were mixed with 20 mL of $RuCl_3.xH_2O$ (1 mmol). The dark brown solutions were neutralized at pH 7-8 by 0.1M of ammonia solution, then refluxed for 3 hrs with continuous stirring. The dark brown precipitates were isolated, washed with few amount of CH_3OH and dried over anhydrous $CaCl_2$. Despite numerous attempts, we were unable to collect any crystals suitable for X-ray structural analyzes.

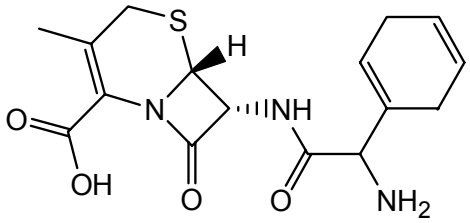

Fig. 1_a – Cefradine (ceph-1) drug.

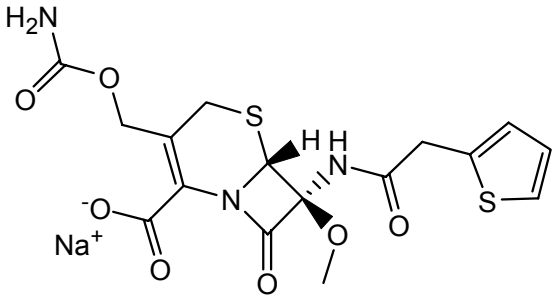

Fig. 1_b – Cefoxitin sodium (ceph-2) drug.

3. Instrumentations

Instrument	Measurement
Perkin Elmer CHN 2400	Contents C, H and N
Jenway 4010 conductivity meter	Electrolytic or non-electrolytic character
Bruker FTIR Spectrophotometer	IR measurements
UV2 Unicam UV/Vis Spectrophotometer	Electronic spectra
Magnetic balance, Sherwood Scientific, Cambridge, England, at Temp 25 ^oC	Magnetic moments
Shimadzu TGA-50H	Thermal analysis
X 'Pert PRO PAN analytical X-ray powder diffraction	X-ray diffraction patterns
Quanta FEG 250 equipment	Scanning electron microscopy (SEM) images
JEOL 100s microscopy	Transmission electron microscopy images (TEM)

4. Biological assessments

4.1. Antimicrobial test

Antimicrobial activity of the ruthenium(III) cephs complexes was screened against Gram (+) (*Staphylococcus epidermidis* and *Staphylococcus aureus*) and Gram(−) (*Klebsiella* spp. and *Escherichia coli*) bacterial strains, using the Kirby-Bauer disc diffusion technique.[22,23] Anti–cancer assessment of the synthesized ruthenium(III) complexes against colorectal adenocarcinoma (Caco-2) and breast cancer (MCF-7) cell lines was performed according to the standard red uptake assay.[24]

RESULTS AND DISCUSSION

1. Physical and analytical results

Two synthesized ruthenium(II) complexes of cefradine (ceph-1) and cefoxitin (ceph-2) have a brown color, stable and homogeneous morphology. These complexes have a melting points above >250 ^{o}C, soluble in (DMF and DMSO) but insoluble in common organic solvents such as (alcohols, ether, benzene, and cyclohexane). Molar conductance values (15-21 $ohm^{-1}cm^{2}mol^{-1}$) of the complexes in DMSO solution indicated that all of the complexes are non-electrolytes,[25] so the location of chloride ions are inside the coordination sphere, this was supported using a $AgNO_3$ reagent. There are three types of coordination regarding cefradine and cefoxitin drugs towards central metal ions as quadridentate (ONON, OONO or OOON), tridentate (ONO, OOO, NNO or NNN) and bidentate (NO, OO, or NN) chelation. The molecular modeling study[26] deduced that no cases of the ligand (ceph-1 or ceph-2) can stereochemically possess as quadridentate or tridentate. The molar ratio between ceph-1 or ceph-2 antibiotic drugs and Ru^{3+} in neutralized media is 1:1 with molecular formula $[Ru(L)(Cl)_2(H_2O)_2]$ where L= ceph-1 or ceph-2. The microanalytical analysis of the two new Ru(III) complexes can be summarized as: [Ru(ceph-1) $(Cl)_2(H_2O)_2$] complex (I, Fig. 2a): $C_{16}H_{22}Cl_2N_3O_6RuS$, Anal. data: Mwt. 556.40 g/mol; color: dark brown; yield: 73%; *Calcd (%)*: C: 34.54; H: 3.99; N: 7.55; Ru: 18.16; Cl: 12.74, *Found (%)*:C: 34.30; H: 3.84; N: 7.46; Ru: 18.08; Cl: 12.55. $[Ru(ceph\text{-}2)(Cl)_2(H_2O)_2]$ (II, Fig. 2b): $C_{16}H_{20}Cl_2N_3O_9RuS$, Anal. data: Mwt. 634.45 g/mol; color: dark brown; yield: 75%; *Calcd (%)*: C: 30.29; H: 3.18; N: 6.62; Ru: 15.93; Cl: 11.18, *Found (%)*:C: 30.12; H: 3.06; N: 6.43; Ru: 15.73; Cl: 11.07.

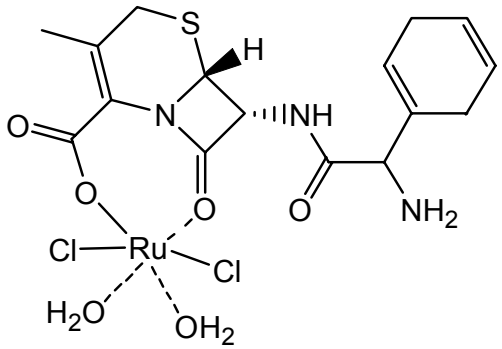

Fig. 2a – Speculated structure of $[Ru(ceph\text{-}1)(Cl)_2(H_2O)_2]$ complex.

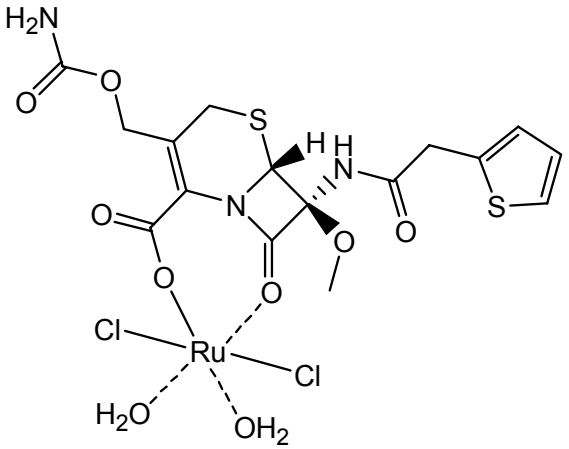

Fig. 2b – Speculated structure of $[Ru(ceph\text{-}2)(Cl)_2(H_2O)_2]$ complex.

2. Infrared spectra results

The FTIR spectra of the two new ruthenium(III) complexes in comparison with the free cefradine and cefoxitin drug ligands are displayed in Fig. 3_{a-d} and summarized in Table 1 with some tentative distinguish assignments [2,7,12]. The IR spectra of the cefradine and cefoxitin shows some characteristic bands at (3347, 3289, 1771 and 1677 cm^{-1}) and (3486, 3289, 1757 and 1677 cm^{-1}) mainly due to the $\nu(NH_2)$, $\nu(NH)$, $\nu(COOH)$ and $\nu(C=O)$ stretching vibrations, respectively.[7-12] The ruthenium(III) complexes included the presented bands of free drug ligand (ceph-1 & ceph-2) and other coordination bands associated after chelation between Ru^{3+} ions and drug ligand. In the IR spectra of the synthetic Ru(III) complexes, the band of carboxylic group (1771-1757 cm^{-1}) are absent while the bands of asymmetrical vibrations $\nu_{as}(COO)$ at 1589-1574 cm^{-1}, and the bands of $\nu_s(COO)$ symmetrical vibrations at 1341-1319 cm^{-1} are present[7] (Table 1). In case of the FTIR spectra of the prepared complexes, the difference between values of ($\nu_{as}COO$-$\nu_s COO$) of the carboxylate groups are similar to the sodium salt, it probably the carboxylate group act as monodentate chelation. Therefore, the carboxyl group is chelated to the ruthenium ion. The band due to $\nu(C=O)$ β–lactam ring at 1677 cm^{-1} was found shifted to lower wavenumber (30-37 cm^{-1}) in the spectra of its Ru^{3+} complexes. A new absorption band at 600-500 cm^{-1} is assigned to $\nu(M-O)$ of COO and CO oxygens. The absence of $\nu(M-N)$ vibration band is confirm the unsharing of the $-NH_2$ group in the coordination with the ruthenium ion.

Table 1
FT-IR assignments of ceph-1 and ceph-2 drugs and its Ru^{3+} complexes (I &II)

Assignments*	Compounds			
	ceph-1	ceph-2	I	II
$\nu(C=O)$; COOH	1771	1757	-	-
$\nu(C=O)$; β-lactam + $\delta(H_2O)$	1677	1677	1640	1647
$\nu_{as}(COO)$	-	-	1574	1589
$\nu_s(COO)$	-	-	1319	1341
$\Delta\nu$	-	-	255	248

* ν_s= stretching symmetry; ν_{as} = stretching asymmetric; δ = bending

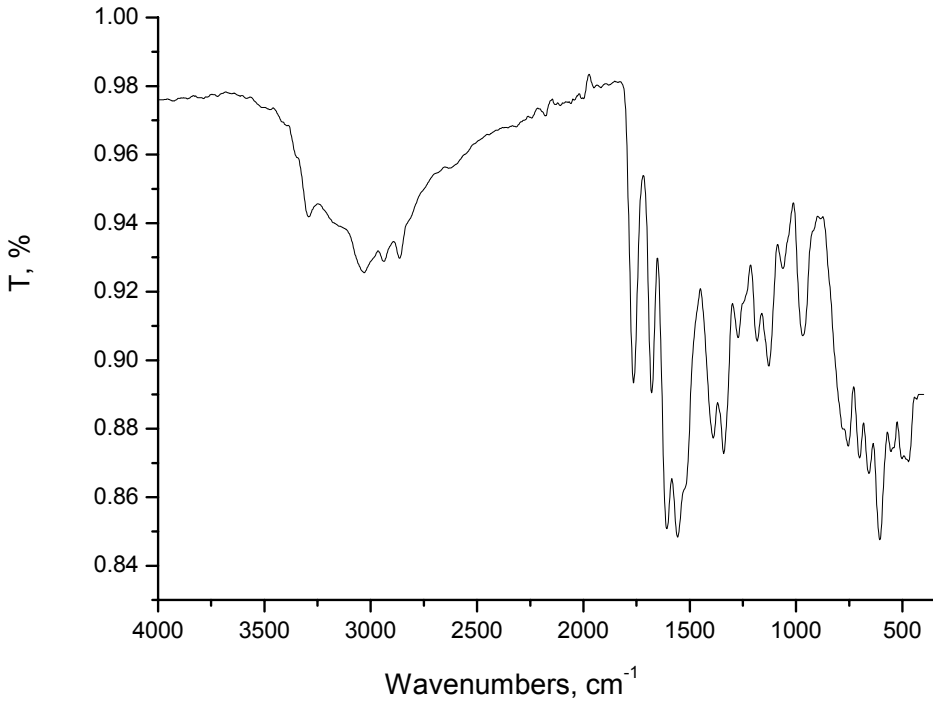

Fig. 3a – FT-IR spectrum of free ceph-1 drug.

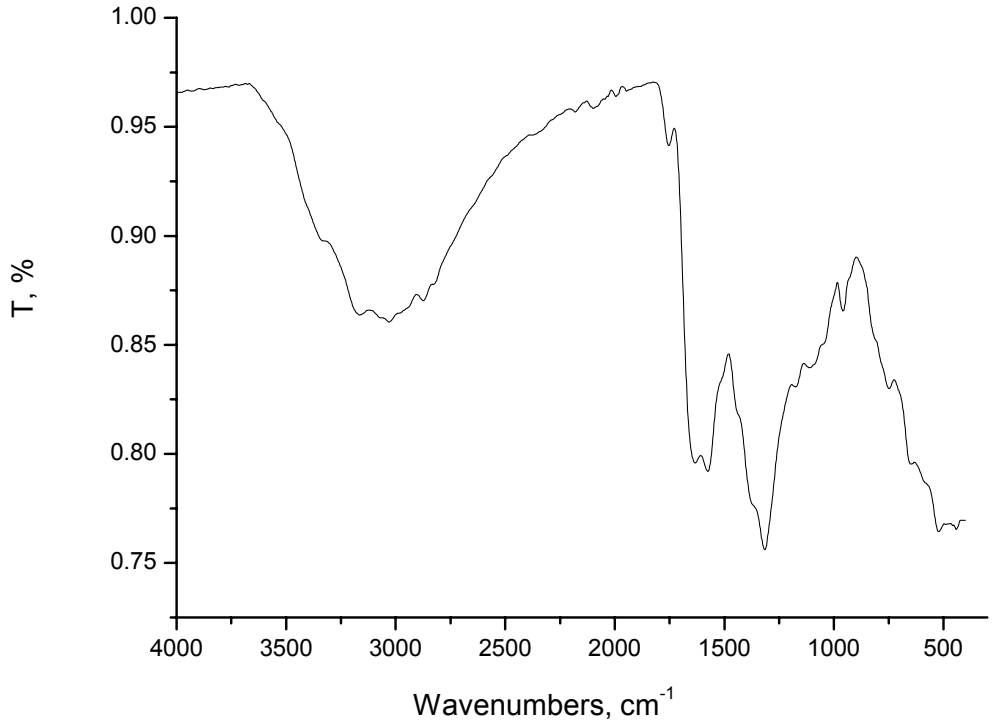

Fig. 3b – FT-IR spectrum of Ru^{3+} ceph-1 complex.

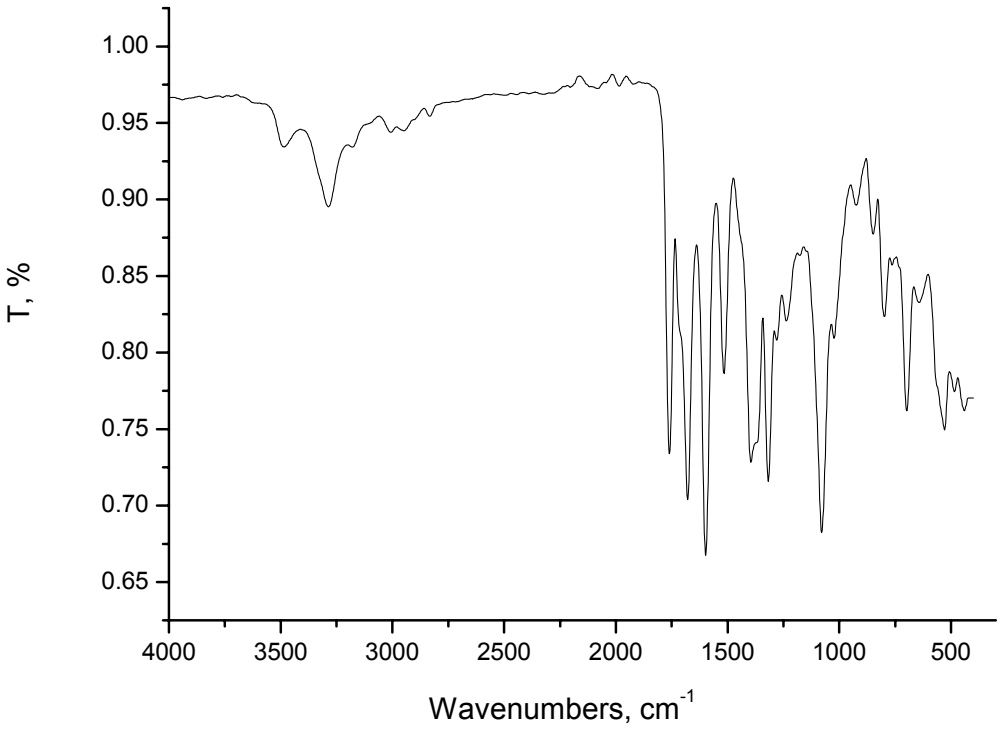

Fig. 3c – FT-IR spectrum of free ceph-2 drug.

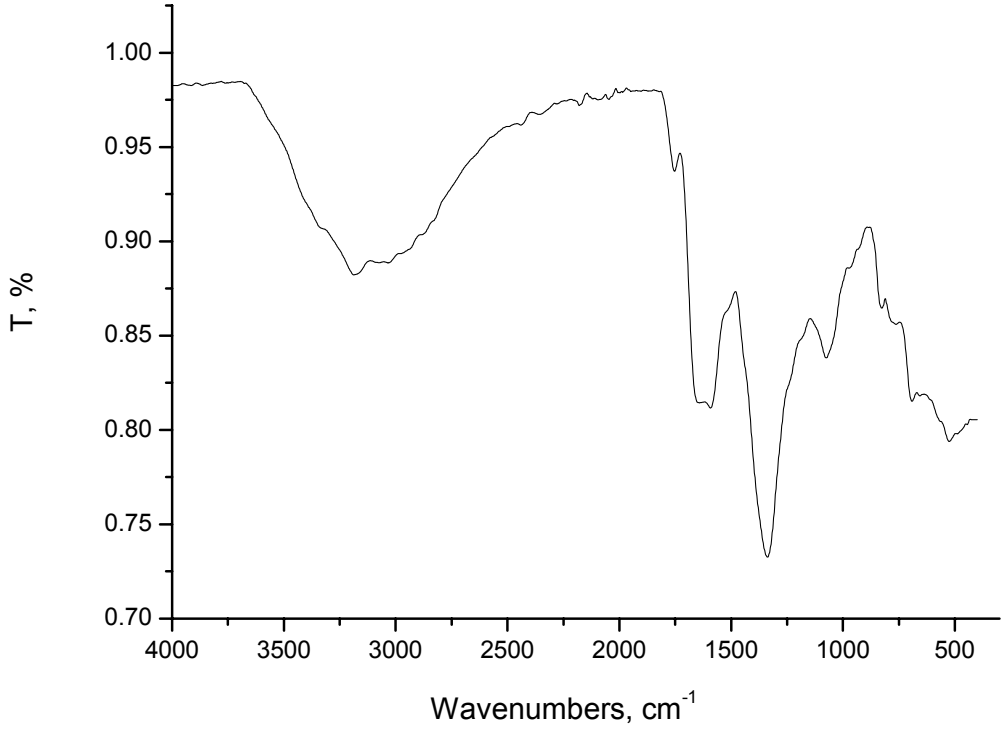

Fig. 3d – FT-IR spectrum of Ru^{3+} ceph-2 complex.

3. Electronic spectra and Magnetic susceptibility results

The UV–Vis spectra of the ruthenium(III) complexes were recorded in DMSO solution at concentration (10^{-3} M). Complexes **I–II** show two absorption bands within the range of 420–440 and 630–650 nm, respectively, attributed to intra-ligand bands. The band within 420–440 nm range may be due to ligand-to-metal charge transfer (L-M_{CT}) transition[27-29] while the bands at 660–680 nm range are assigned to spin allowed $^1A_{1g}\rightarrow{}^1T_{1g}$ transition.[27,28] The d–d transition bands $^2T_{2g}\rightarrow{}^4T_{1g}$, $^2T_{2g}\rightarrow{}^4T_{2g}$ and $^2T_{2g}\rightarrow{}^2T_{1g}$ are masked by strong L-M_{CT} bands.[29] The Ru^{3+} metal ions is one of the second transition metal series, which it is always has a low spin with μ_{eff} 1.80 B.M.[30] The μ_{eff} values for the two synthesized ruthenium(III) complexes located within the range of 1.74–1.78 B.M. with octahedral configuration (d^5 & S = ½).[31] Therefore, the μ_{eff} values for these complexes are in accord with the (+3) oxidation of ruthenium.

4. Thermogravimetric(TGA/DTA) and kinetic results

The TGA and DTA curves of the free cefradine and cefoxitin sodium drug ligands are shown in Fig. 4(A&B). Three dissociation stages of both ceph-1 and ceph-2 ligands are detected in TGA and DTA curves. The thermal cracking beginning from 25 °C and ends at 800 °C, the observed mass losses for the ceph-1 and ceph-2 are 100% and 84.95% against calculated 100% and 85%, respectively, these are corresponding to the release of $C_{16}H_{19}N_3O_4S$ and $C_{16}H_{16}N_3O_7S_2$ molecules. The results shown that the final product of cefoxitin sodium drug ligand is considered to be Na_2O. In case of cefradine ligand, there is one endothermic peak (467 °C) and two exothermic peaks (215 and 595 °C) but concerning the cefoxitin sodium drug, it contains a three exothermic peaks at 265, 447, 592 °C in DTA curves due to the chemical events existed in the TGA curves.

TGA and DTA curves of [Ru(ceph-1)$(Cl)_2(H_2O)_2$] complex are displayed in Fig. 4C. The TG and DTA curves display the decomposition of Ru^{3+} ceph-1 complex in three thermal dissociation endothermic peaks at 148, 442, and 666 °C. The mass loss observed is 82%, showing that organic group ($C_{16}H_{22}Cl_2N_3O_6S$) is released. The experiment result is similar to the decomposition of the first complex. The final product is considered to be ruthenium metal polluted with few carbon atoms. The TGA and DTG curves of [Ru(ceph-2)$(Cl)_2(H_2O)_2$] complex are shown in Fig. 4D. One endothermic peak (134 °C) and two exothermic peaks at 342 and 708 °C are observed in the DTA

curve. The first-to-third decomposition stages have a mass loss observed is 73% against the calculated loss of 73.96%, due to the release of one molecule of ceph-2, chlorine gas and two molecules of H_2O. The final product is considered to be RuS_2 polluted with few carbon atoms. Thermal stability of [Ru(ceph-2)$(Cl)_2(H_2O)_2$] complex is more than [Ru(ceph-1)$(Cl)_2(H_2O)_2$] complex. The final product of the two synthesized ruthenium(III) complexes indicted that the different metal ion interaction is exist in coordination environment, because the ruthenium ion changed oxide with heating.

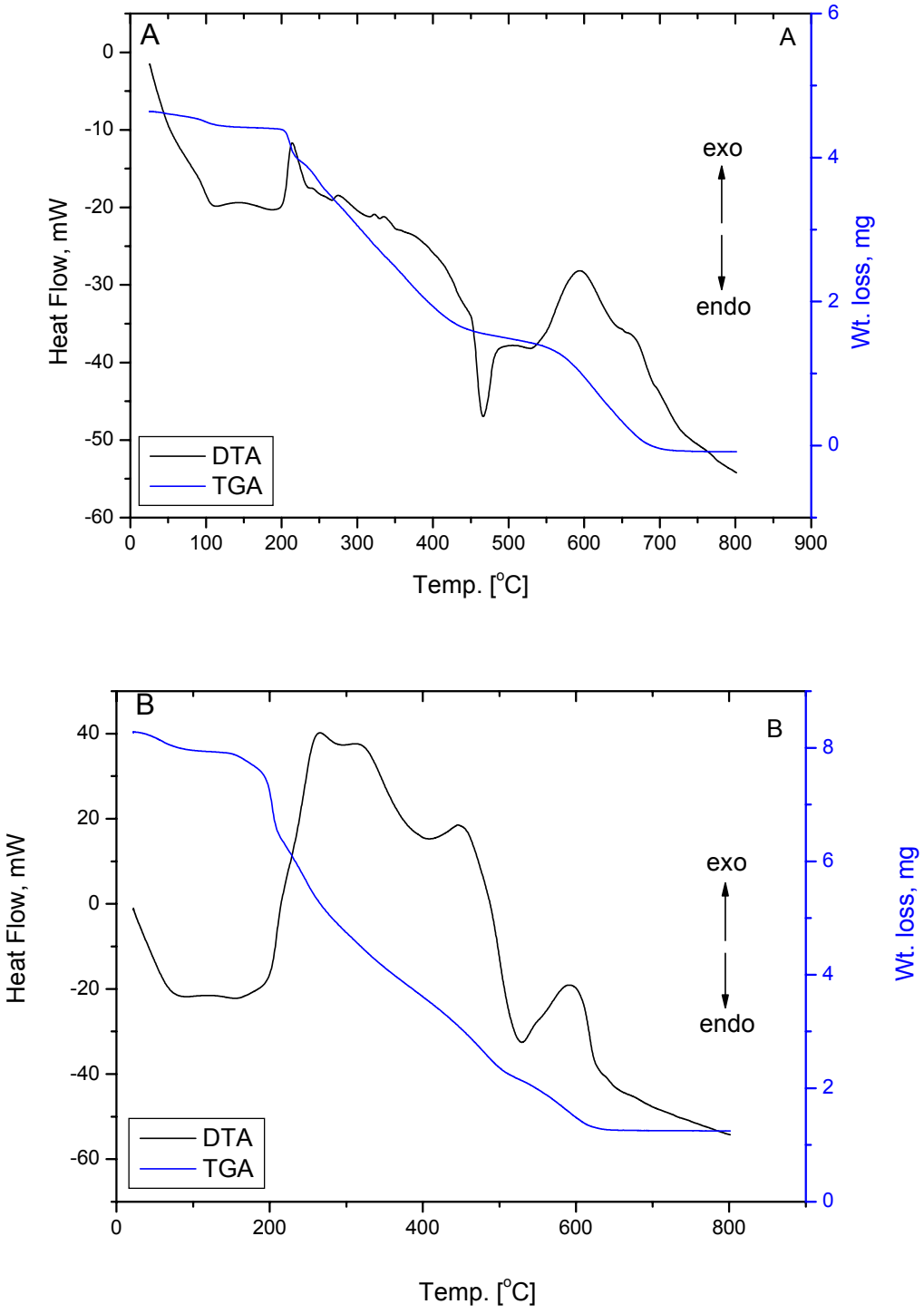

Fig. 4 (A&B).

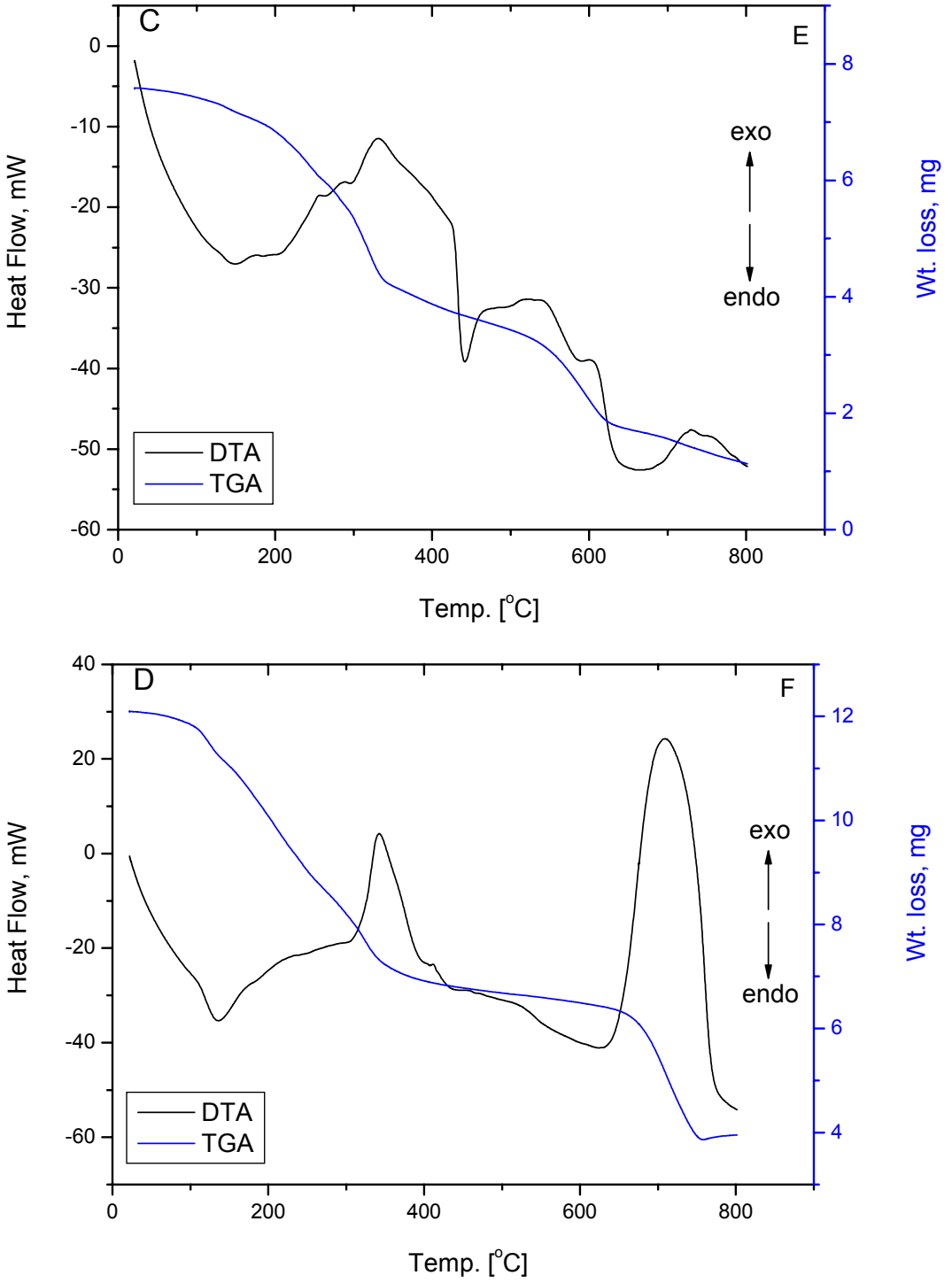

Fig. 4 – TGA and DTA curves of (A): ceph-1 drug, (B): ceph-2 drug, (C): Ru^{3+} ceph-1 complex and (D): Ru^{3+} ceph-2.

Kinetic thermodynamic parameters (E*, Z, ΔS*, ΔH*, ΔG*) were calculated based on two non-isothermal decomposition methods of Coats-Redfern[32] and modified Horowitz-Metzger[33] as listed in Table 2 and displayed in Fig. 5.

Table 2 refer to the kinetic data collected from TG curves, it was found that all compounds have a negative ΔS values except for [Ru(ceph-2)$(Cl)_2(H_2O)_2$] complex, due to the higher ΔH value. The greater the thermal stability of a complex, the higher value of the activation energy (E*) for decomposition.[34]

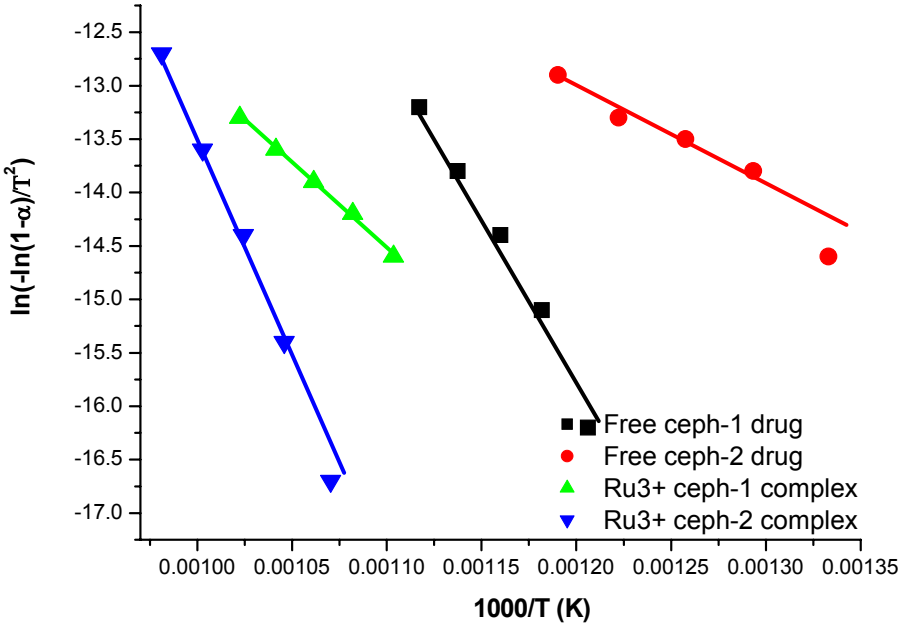

Fig. 5A

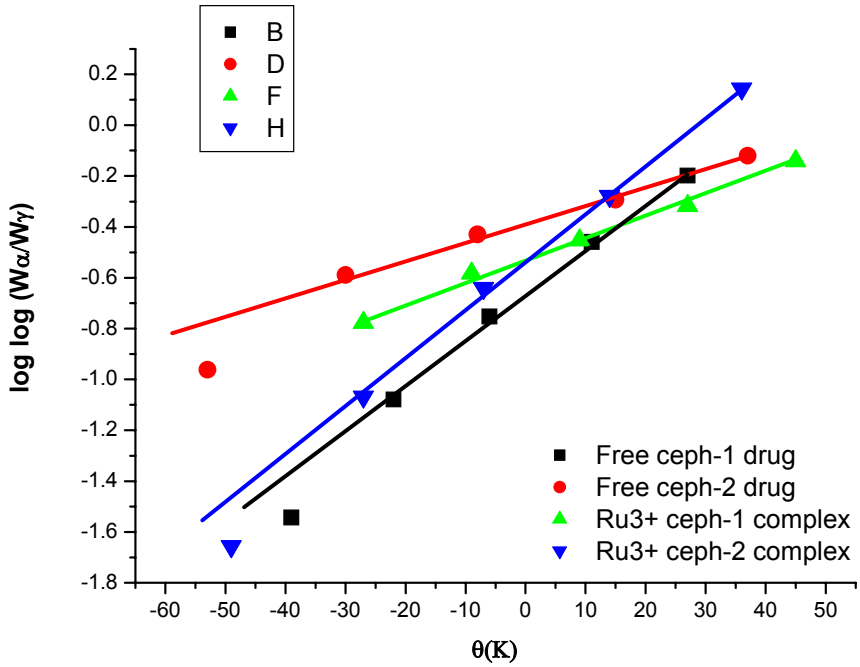

Fig. 5B

Fig. 5 – Kinetic curves of ceph-1 drug, ceph-2 drug, Ru^{3+} ceph-1 complex and Ru^{3+} ceph-2 complex by (A): Coats-Redfern (B): Horowitz-Metzger non-isothermal methods.

Table 2

Kinetic thermodynamic parameters based on Coats-Redfern (CR) and Horowitz-Metzger (HM)

Compound	Methods	Parameters					r
		E (J mol^{-1})	A (s^{-1})	ΔS (J mol^{-1} K^{-1})	ΔH (J mol^{-1})	ΔG (J mol^{-1})	
Ceph-1	CR	2.74E+05	1.60E+14	-1.81E+01	2.67E+05	2.51E+05	0.99369
	HM	2.90E+05	3.09E+15	-4.27E+01	2.82E+05	2.45E+05	0.99382
Ceph-2	CR	9.15E+04	3.47E+03	-1.85E+02	8.48E+04	2.34E+05	0.97322
	HM	1.09E+05	6.06E+04	-1.62E+02	1.02E+05	2.32E+05	0.97702

Table 2 (continued)

Ru ceph-1	CR	1.31E+05	6.70E+04	-1.62E+02	1.23E+05	2.75E+05	0.9990
	HM	1.42E+05	4.59E+05	-1.46E+02	1.35E+05	2.71E+05	0.99751
Ru ceph-2	CR	3.68E+05	2.78E+17	7.91E+01	3.60E+05	2.82E+05	0.99754
	HM	3.85E+05	3.40E+18	9.99E+01	3.77E+05	2.79E+05	0.99611

[a] Units of parameters: E in kJ mol^{-1}, A in s^{-1}, ΔS in J mol^{-1}K^{-1}, ΔH and ΔG in kJ mol^{-1}.

5. X-ray powder diffraction, SEM and TEM results

Figure 6 shows the XRD pattern of the solid powder [Ru(ceph-1)$(Cl)_2(H_2O)_2$] and [Ru(ceph-2) $(Cl)_2(H_2O)_2$] complexes. The particles size and crystallinity are discussed based on full width at half maximum peak using Debye-Scherer's equation.[35] The particle size of the tested samples is inserted between 14-20 nm. XRD of the Ru^{3+} complexes included three characteristic reflection peaks at ~31, 44, and 52° attributed to (002), (100), and (101) planes regarding ruthenium metal.[36] It is observed that crystalline size is different for both the complexes, due to change in the cefradine and cefoxitin drug positions.

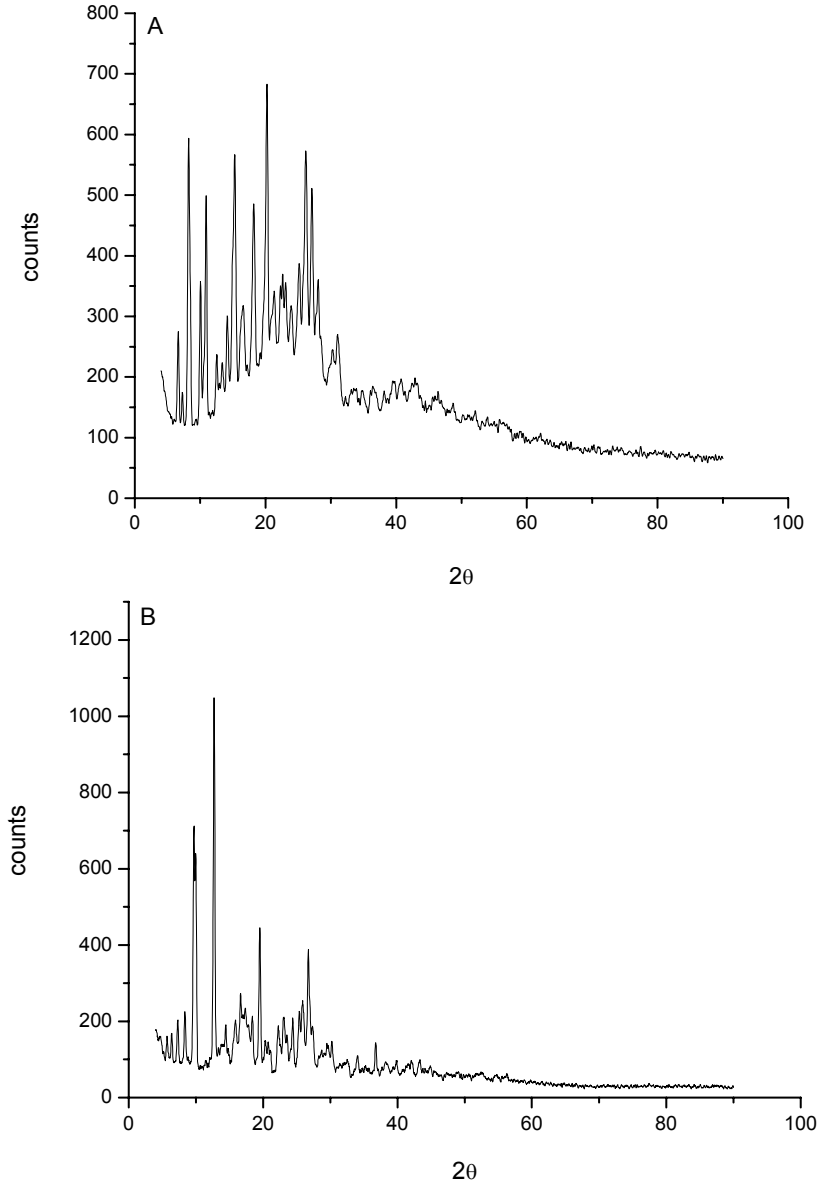

Fig. 6 – XRD patterns spectrum of the (A): Ru^{3+} ceph-1 and (B): Ru^{3+} ceph-2 complexes.

A

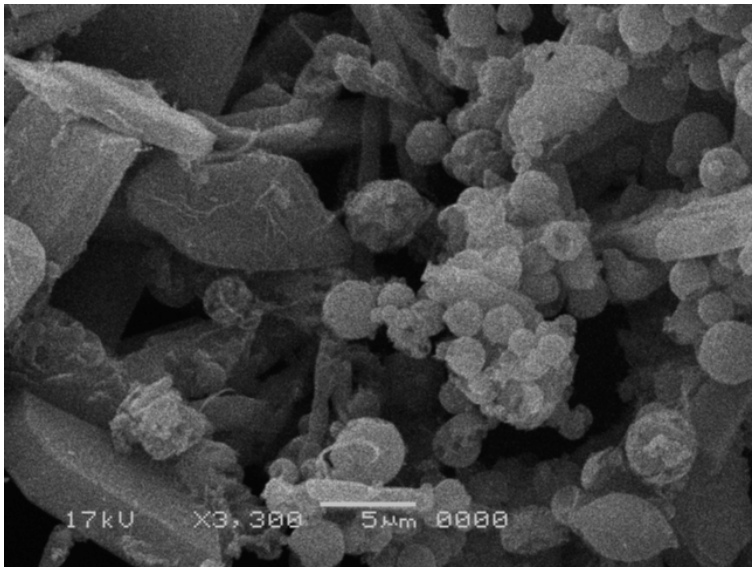

B

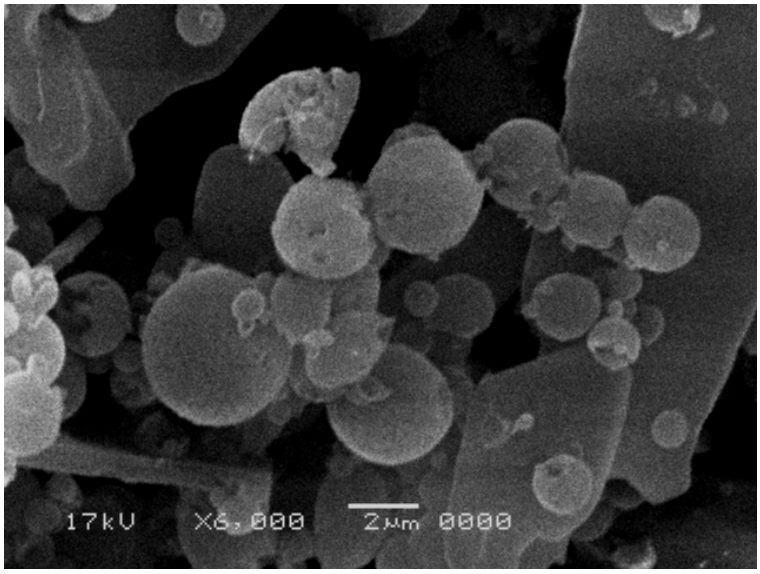

Fig. 7 – SEM images of (A): Ru^{3+} ceph-1 and (B): Ru^{3+} ceph-2 complexes.

The SEM images of the two Ru^{3+} complexes are displayed in Fig. 7. From this figure it can be shown that the average length of grain sizes of the Ru^{3+} ceph-1 and Ru^{3+} ceph-2 complexes are 2-5 μm, respectively. The surface morphology changes with change in structure of drug ligand, both two images have large number of irregular shaped and some included a regular spherical grain associated with the images refereed in Fig. 7. It is quite clear from SEM results that the average grain size calculated from SEM are quite larger than the average grain size estimated from XRD analysis.

The transmission electron microscopy (TEM) images of Ru^{3+} ceph-1 and Ru^{3+} ceph-2 complexes have been given in Fig. 8. The size of the nanoparticles obtained from the XRD diffraction patterns are in close agreement with the TEM studies which show sizes of about 10-20 nm, which shows the good crystalinity of the nanoparticles.

6. Biological results

The comparison of the antibacterial activity of free cefradine and cefoxitin drug ligands with that of ruthenium(III) complexes against different bacterial strains (Table 3), it was found that the cefradine and cefoxitin–Ru^{3+} complexes have a better biological activity than the free drug ligands. These results can be traced to the active role of the ruthenium metal in increasing the biological efficacy of the drug ligands, due to its ability to penetrate the bacterial cells.[37-40]

A

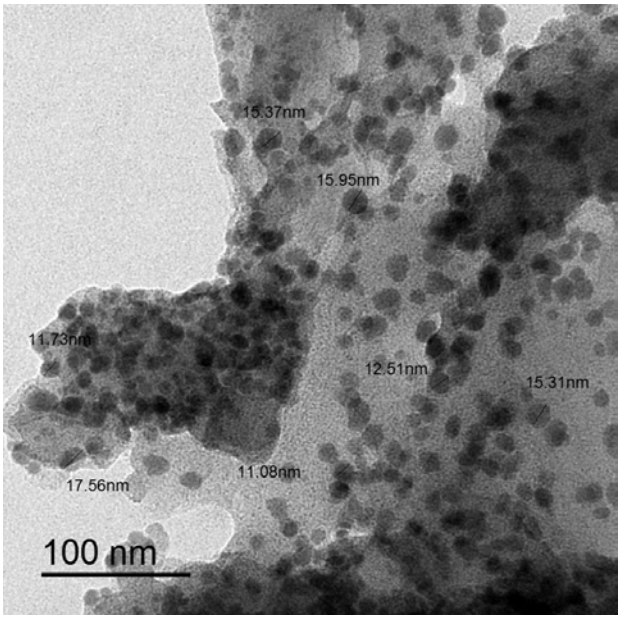

B

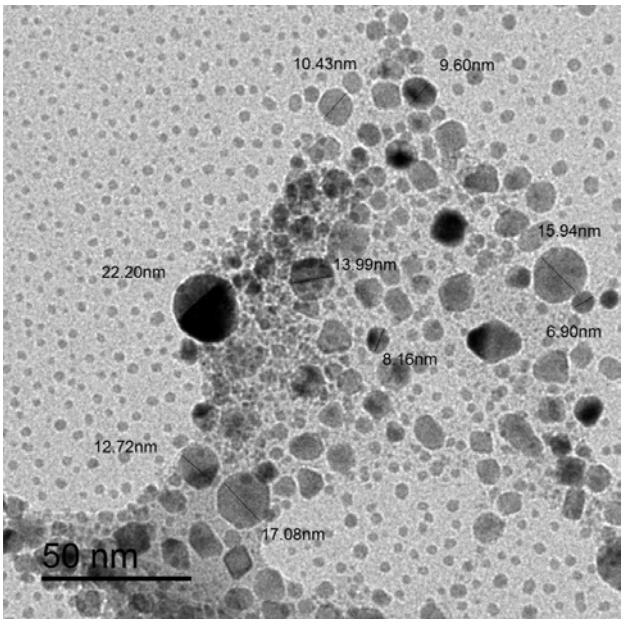

Fig. 8 – TEM images of (A): Ru^{3+} ceph-1 and (B): Ru^{3+} ceph-2 complexes.

Table 3

Growth inhibition zone (mm) of ceph-1 drug, ceph-2 drug, Ru^{3+} ceph-1 complex and Ru^{3+} ceph-2 complex

Sample	**Inhibition zone diameter (mm)**			
	Bacteria			
	***Staphylococcus epidermidis*, (G^+)**	***Staphylococcus aureus*, (G^+)**	***Klebsiella* spp.(G^-)**	***Escherichia coli*, (G^-)**
Control: DMSO	0.0	0.0	0.0	0.0
Tetracycline Standard drug	27	26	29	25
Control (DMSO)	0.0	0.0	0.0	0.0
ceph-1	26	24	27	28
Ru^{3+} ceph-1	28	25	26	29
ceph-2	25	26	24	27
Ru^{3+} ceph-2	28	29	26	25

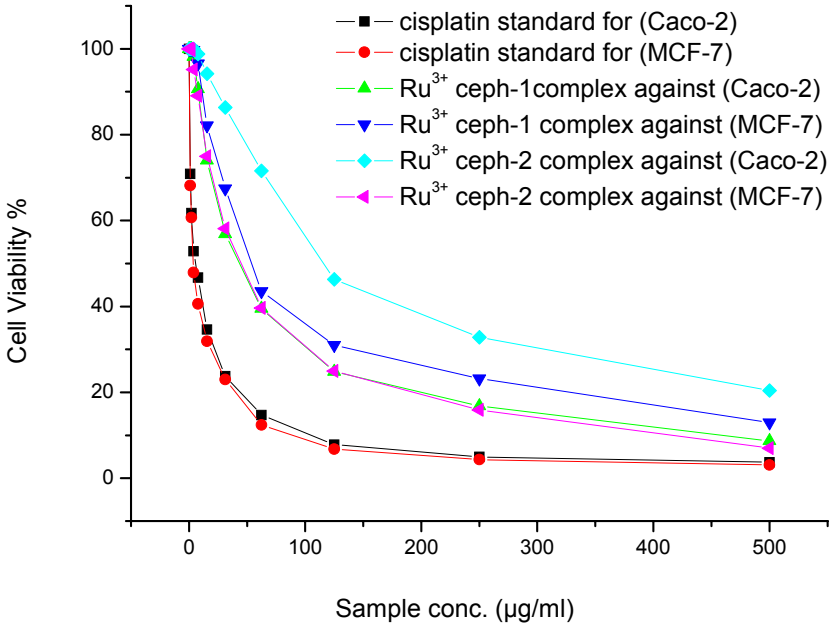

Fig. 9 – Relationship between sample concentration
and cell viability of Ru^{3+} complexes and cisplatin against (Caco-2) and (MCF-7) cancer cell lines.

The anticancer activities of ruthenium(III) complexes of ceph-1 and ceph-2 drugs against the colorectal adenocarcinoma (Caco-2) and breast cancer (MCF-7) cell lines are shown in Fig. 9. The % cell inhibition and IC_{50} values (43.6, 54, 116, and 45 µg/mL) for the Ru^{3+} ceph-1complex against (Caco-2), Ru^{3+} ceph-1 complex against (MCF-7), Ru^{3+} ceph-2 complex against (Caco-2) and Ru^{3+} ceph-2 complex against (MCF-7) (figure 9) indicate that ruthenium(III) complexes have an efficacy towards the Caco-2 and MCF-7 cancer lines comparable with cisplatin standard drug (5.71 and 3.67 µg/mL).

CONCLUSION

The availability of chemical and biological data presented in this paper is the basis for understanding not only the current state of anti-cancer drugs based on ruthenium(III), but also the rationale for strategies for future drug design. New Ru(III) nanosized complexes of cefradine and cefoxitin were synthesized. Ruthenium(III) complexes were discussed based on the elemental, molar conductance, thermal and magnetic moment measurements as well as spectral (FTIR, UV–Vis, and XRD) techniques. FT-IR spectra revealed that the ligands reacted as a bidentate ligands through carboxylate oxygen and β-lactam oxygen groups. The analytical analysis confirmed that the molar ratio is 1:1 (Ru^{3+}/ceph). In *vitro* antimicrobial activities of Ru(III) complexes were evaluated towards G+ & G– bacteria. The antitumor activities of Ru(III) complexes are appraised against breast (MCF-7) and colorectal adenocarcinoma (Caco-2) cell lines, which means that the two complexes may be considered promising antimicrobial and anticancer drugs.

Acknowledgements. This research was funded by the Deanship of Scientific Research at Princess Nourah bint Abdulrahman University, through the Research Funding Program (Grant No. # RFP-1440-3).

REFERENCES

1. A.R. Ribeiro, B. Sures and T.C. Schmidt, *Environmental Pollution*, **2018,** *241*, 1153-1166.
2. C. García-Estrada and J.-F. Martín, "Comprehensive Biotechnology", Third edition, Volume 3, 2019, p. 283-296.
3. D. B. Sunjaya, R. J. Lennon, V. H. Shah, P. S. Kamath, D. A. Simonetto, *Mayo Clinic Proceedings*, **2019**, *94*, 1499-1508.
4. D. Kalman and S. L. Barriere, *Tex. Heart Inst. J.*, **1990**, *17*, 203–215.
5. J. R. Anacona and A. Rodriguez, *Trans. Met. Chem.*, **2005**, *30*, 897–901.
6. J. R. Anacona and C. C. Gil, *Trans. Met. Chem.,* **2005**, *30*, 605–609.
7. M. A. Zayed and S. M. Abdallah, *Spectrochim Acta Part A*, **2004**, *60*, 2215–2224.
8. Z. H. Chohan, *Chem. Pharm. Bull.*, **1991**, *39*, 1578–1580.
9. J. R. Anacona and C. C. Gil, *Trans. Met. Chem.,* **2006**, *31*, 227–231.

10. R. M. Yszczek, *J. Therm. Anal. Calorim.*, **2004**, *78*, 473–486.
11. J. R. Anacona and F. Acosta, *J. Coord. Chem.*, **2005**, *59*, 621–627.
12. Z. H. Chohan and C. T. Supuran, *J. Enz. Inhib. Med. Chem.*, 2005, *20*, 463–499.
13. N. Abo El-Maali, A. H. Osman, A. A. M. Aly and G. A. A. Al-Hazmi, *Bioelectrochem*., **2005**, *65*, 95–104.
14. J. R. Anaconaa and J. R. Rodriguez, *J. Coord. Chem.*, **2004**, *57*, 1263–1270.
15. A. A. Abdel Gaber, O. A. Farghaly, M. A. Ghandour and H. S. El-Said, *Monatsh. Chem.*, **2000**, *131*, 1031–1036.
16. J. R. Anacona and P. Alvarez, *Trans. Met. Chem.*, **2002**, *27*, 856–564.
17. R. Kato, K. Ooi, K. Takeda, K. Mashimo, Y. Fujimura, M. Kusumoto and K. Ueno, *Drug Metab. Pharmacokinet*, **2002**, *17*, 363–370.
18. A. Dimitrovska, B. Andonvska and K. Stojanoski, *Int. J Pharm.*, **1996**, *134*, 213–218.
19. S. Page, *Educ. Chem.*, **2012**, *10*, 26–29.
20. C. S. Allardyce and P. J. Dyson, *Dalton Trans.*, **2016**, *45*, 3201–3209.
21. M. I. Webb and C. J. Walsby, *Dalton Trans.*, **2015**, *44*, 17482–17493.
22. A.W. Bauer, W. A. Kirby, C. Sherris and M. Turck, *Am. J. Clin. Pathology*, **1996**, *45*, 493–498.
23. M. A. Pfaller, L. Burmeister, M. A. Bartlett and M. G. Rinaldi, *J. Clin. Microbiol.*, **1988**, *26*, 1437–1442.
24. G. Repetto, A. del Peso and J. L. Zurita, *Nature Protocols*, **2008**, *3*, 1125-1131.
25. M. S. Refat, *Spectrochimica Acta Part A,* **2007**, *68*, 1393–1340.
26. Z. H. Chohan and M. F. Jaffery, *Metal Based Drugs*, **2000**, *7*, 265-269.
27. Y. Tanabe and S. Sugano, *J. Phys. Soc.*, **1954**, *9*, 766-772.
28. S. Chandra, *Synth. React. Inorg. Met.-Org., Nano-Met. Chem.,* **1992**, *22*, 1565–1570.
29. A. B. Lever, "Inorganic Electronic Spectroscopy", Elsevier, Amsterdam, 1968.
30. B. N. Figgis, "Introduction to Ligand Field Theory", 1st edition, Interscience Publishers, New York, p. 287.
31. F. A. El-Saied, R. M. El-Bahnasawy, M. Abdel-Azeem and A. K. El-Sawaf, *Polyhedron*, **1994**, *13*, 1781–1786.
32. A. W. Coats and J. P. Redfern, *Nature* (London), **1964,** *201*, 68-74.
33. H. H. Horowitz and G. Metzger, *Anal. Chem.*, **1963**, *35*, 1464–1469.
34. M. Olszak-Humienik and J. Mozejko, *Thermochimica Acta*, **2000**, *344*, 73–78.
35. A. L. Patterson, *Phys. Rev.*, **1939**, *56*, 978–984.
36. J. P. Singh, T. Karabacak, P. Morrow, S. Pimanpang, T.-M. Lu and G.-C. Wang, J. Nanoscie. Nanotech., **2007**, *7*, 2192–2197.
37. M. Tumer, D. Ekinci, F. Tumer and A. Bulut, *Spectrochimica Acta A*, **2007**, *67*, 916–920.
38. M. Muthukumar and P. Viswanathamurthi, *J. Coord. Chem.*, **2010**, *63*, 1263–1268.
39. Z. Tohidiyan, I. Sheikhshoaie and M. Khaleghi, *Int. J. Nanodimens.*, **2016**, *7*, 127–132.
40. N. Farrell, *Coord. Chem. Rev.*, **2004**, *232*, 1–6.